HHS Public Access

Author manuscript

Lebensm Wiss Technol. Author manuscript; available in PMC 2024 August 08.

Published in final edited form as:

Lebensm Wiss Technol. 2024 July 15; 204: . doi:10.1016/j.lwt.2024.116420.

Innovative application of CRISPR for eliminating Ustiloxin in *Cordyceps militaris*: Enhancing food safety and quality

Mengqian Liu[a,b], **Anning Wang**[a,b], **Guoliang Meng**[a,b], **Qing Liu**[a,b], **Ying Yang**[a,b], **Min Wang**[c], **Zheng Wang**[d], **Fen Wang**[a,**], **Caihong Dong**[a,*]

[a]State Key Laboratory of Mycology, Institute of Microbiology, Chinese Academy of Sciences, Beijing, 100101, China

[b]University of Chinese Academy of Sciences, Beijing, 100049, China

[c]School of Biotechnology and Health Sciences, Wuyi University, Jiangmen, 529020, Guangdong, China

[d]Department of Biostatistics, Yale School of Public Health, New Haven, CT, 06510, United States

Abstract

Cordyceps militaris (L.) Fr. Has long been recognized as a valuable functional food consumed in numerous countries. However, biosynthetic gene clusters of this species and safety regarding mycotoxin production remain largely unexplored. In this study, a ribosomally synthesized and post-translationally modified peptide (RiPP) cluster responsible for the production of cyclopeptide mycotoxins in *Cordyceps* was unveiled via genome mining. Ustiloxin B and a novel, predominant and *Cordyceps* specific ustiloxin I were confirmed by extraction and structural analysis. The difference between Ustiloxins I and B lied in the side chain at C19, where an additional methyl substituent in Ustiloxin I resulted in an alanine moiety substitution for glycine of Ustiloxin B. The simultaneous deletion of the two adjacent core genes, *CmustYb* and *CmustYa*, using a single guide RNA designed in the intergenic region, and subsequent *in-situ* complementation via AMA-mediated CRISPR/Cas9 system confirmed the RiPP cluster's responsibility for ustiloxin production. The cultivation of the edited strain yielded ustiloxin-free fruiting bodies without affecting agronomic characters. PCR and genome resequencing confirmed the absence of any

*Corresponding author. State Key Laboratory of Mycology, Institute of Microbiology, Chinese Academy of Sciences, NO.3 Park 1, Beichen West Road, Chaoyang District, Beijing, 100101, China. dongch@im.ac.cn (C. Dong). **Corresponding author. State Key Laboratory of Mycology, Institute of Microbiology, Chinese Academy of Sciences, NO.3 Park 1, Beichen West Road, Chaoyang District, Beijing, 100101, China. wangfen@im.ac.cn (F. Wang).

CRediT authorship contribution statement

Mengqian Liu: Writing – review & editing, Writing – original draft, Validation, Methodology, Investigation, Formal analysis, Data curation, Conceptualization. **Anning Wang:** Methodology, Investigation, Data curation. **Guoliang Meng:** Software, Investigation, Formal analysis, Data curation. **Qing Liu:** Methodology, Investigation, Data curation. **Ying Yang:** Investigation, Funding acquisition, Data curation. **Min Wang:** Validation, Methodology. **Zheng Wang:** Writing – review & editing, Investigation, Funding acquisition. **Fen Wang:** Writing – review & editing, Methodology, Investigation, Data curation, Conceptualization. **Caihong Dong:** Writing – review & editing, Supervision, Methodology, Funding acquisition, Conceptualization.

Declaration of competing interest

The authors declare that they have no known competing financial interests or personal relationships that could have appeared to influence the work reported in this paper.

Appendix A. Supplementary data

Supplementary data to this article can be found online at https://doi.org/10.1016/j.lwt.2024.116420.

off-target events or foreign sequence remnants. This study marks a significant advancement in utilizing CRISPR technology to control ustiloxins in food, underscoring its broader implications for food safety and quality improvement.

Keywords

Cordyceps ; RiPP cluster; Ustiloxin; CRISPR/Cas9; Ustiloxin elimination

1. Introduction

Cordyceps militaris (L.) Fr. is a valuable edible fungus that has been widely used as a functional and healthy food in many countries, especially in East Asia. It has been listed as a novel food by Chinese government (Ministry of Health of the People's Republic of China, 2009). Mass production of fruiting bodies and manufactory fermentation of mycelium of *C. militaris* have long been successful to satisfy the large demand for medicinal and nourishment purposes (Chen et al., 2020).

As a type of raw materials of functional food, *C. militaris* has attracted increasing attention. Nucleosides and analogues (Cunningham et al., 1950), carotenoids (Yan et al., 2010) and polysaccharides (Zhang et al., 2019) are the main components identified in *C. militaris*. Using the online genome mining platform, antiSMASH (Blin et al., 2021), 30 putative biosynthetic gene clusters (BGCs) were predicted in *C. militaris* CM01 genome (Zheng et al., 2011). However, only a small fraction of BGCs have been analyzed, including a PKS-NRPS hybrid responsible for beauveriolides (Wang et al., 2020), and a PKS for cordypyrone A and B (Gao et al., 2022). Recently, three *C. militaris* genes (*CCM_02059, 02060,* and *02061*) of one RiPP (ribosomally synthesized and post-translationally modified peptide) cluster were reported to share a sequence similarity of over 50% (with a coverage over 50% and E value of $< 1\ E^{-18}$) with *Aspergillus flavus* genes *AFLA_094990* and *AFLA_094960* in a gene cluster that has been confirmed to be responsible for the ustiloxin B biosynthesis (Zhang et al., 2022). Given possible conserved functions among homologous gene clusters, the RiPP cluster may be play roles in biosynthesis of ustiloxin-related compounds in *C. militaris*.

Ustiloxins are cyclopeptide mycotoxins originally discovered from rice false smut balls (FSBs) infected by the fungal pathogen *Ustiaginoidea virens* (Koiso et al., 1992). To date, eight kinds of ustiloxins have been isolated and identified from FSBs and designated as ustiloxin A-H (Koiso et al., 1994, 1998; Wang et al., 2017; Ye et al., 2016). Ustiloxins were reported to be toxic to both plants and animals by inhibiting microtubule assembly and cell skeleton formation, and among all known ustiloxins, ustiloxin A was considered as the most toxic derivative (Ladhalakshmi et al., 2012).

Safety assessments on *C. militaris* consumption have revealed no toxic effect for the usage of fruiting body at the dose of 3000 mg/kg/day (Jędrejko et al., 2021) or fermented mycelium at 4000 mg/kg/day in rats in the subacute oral toxicity tests (Jhou et al., 2018). However, toxic effects *C. militaris* were reported in some studies. In acute toxicity tests, moderate doses of *C. militaris* tissue (45 mg/100 g per day) were given gavage three

times a day, and the mice exhibited significant symptoms of being poisoned, including death, lower behavioral activity, and significant weight loss compared with blank controls (Song et al., 2018). In a subacute oral toxicity test, high doses (125 mg/100 g per day) of *C. militaris* exhibited significant toxic effects in mice. These effects included depressed mental behavior, reduced body weight compared to the control group, severe damage to vital organs such as the kidney and liver, and even mortality (Song et al., 2018). In human studies, *C. militaris* supplementation did not correlate with the occurrence of serious adverse events, however, a few of the mild adverse events with gastrointestinal disturbances were reported (Dudgeon et al., 2018). To ascertain whether *C. militaris* can produce ustiloxins, cyclopeptide mycotoxins, is critical for the *Cordyceps* industry.

Given the increasing demand for food resources with improved properties, CRISPR-enabled engineering technology has been widely applied to commercial and model crops to increase yield and improve the nutritional properties and quality (Barrangou & Doudna, 2016). In many countries, including the USA and Japan, transgene-free gene-edited crops are treated as conventional crops and are exempt from the restrictive government policies tailored for transgenic crops (Zhu, 2022). In China, the Ministry of Agriculture and Rural Affairs issued a guideline for the regulatory approval of gene-edited crops in 2022, paving the way for commercialization of this important breeding technology of CRISPR-enabled engineering. Along with the first gene-editing biosafety certificate has been approved in China on April 28th, 2023, the commercial value of gene-editing foods will undoubtedly promote the application of gene editing technology in variety improvement.

Recently, an effective AMA1-based CRISPR/Cas9 system for highly efficient marker-free gene deletion via homology-directed repair (HDR) was successfully constructed in *C. militaris* (Meng et al., 2022), facilitating the application of the CRISPR/Cas9 technology in quality improvement in this mushroom.

In the present study, a RiPP cluster associated with ustiloxins was first predicted in the genome of *C. militaris*. Subsequently, ustiloxin B and a novel ustiloxin were confirmed by extraction and structure elucidation. Further, CRISPR/Cas9 mediated deletion and complement of the core genes confirmed that this BGC was responsible for the production of ustiloxin in *C. militaris*, and ustiloxin-free fruiting bodies of *C. militaris* were obtained through cultivation with the edited strain. The off-target events and residual of foreign sequences were excluded by PCR and genome resequencing. Besides, ustiloxin production was detected in some species of *Cordyceps* s.l. The study aimed to identify and confirm the RiPP cluster associated with ustiloxin production in *C. militaris* and enhance the safety and quality of this edible fungus by eliminating ustiloxin production. This was achieved using an effective AMA1-based CRISPR/Cas9 system for precise, marker-free gene deletion via homology-directed repair (HDR). This work highlights the broader implications of the CRISPR/Cas9 system for improving food safety and quality.

2. Materials and methods

2.1. Strains and fruiting body cultivation

Cordyceps militaris strain CGMCC 3.16320, *Beauveria bassiana* strain CGMCC 3.3575, *Beauveria brongniartii* strain 302, *Cordyceps fumosorosea* strain 1579 and *Metarhizium robertsii* strain ARSF23 were maintained on potato dextrose agar (PDA) medium at 4 °C. The specimens of *Ophiocordyceps sinensis* and *Cordyceps chanhua* were collected from Tibet, and Jiangsu provinces, respectively and kept at the State Key Laboratory of Mycology, Institute of Microbiology, Chinese Academy of Sciences. All strains for fruiting were cultivated in wheat medium or pupae of *Antheraea pernyi*. For the cultivation on *A. pernyi*, 8×10^5 conidia per pupa were injected. Biological efficiency (BE, %) was defined as the percentage of dry weight of harvested fruiting body over dry weight of substrate (Zhang et al., 2018).

2.2. Identification of the putative BGCs of ustiloxin from genome of Cordyceps s.l

A BLASTP search (expect threshold = 0.05; word size = 5; max matches in a query range = 0; matrix = BLOSUM62) was performed against the *C. militaris* genome of strain CM01 (GenBank: GCA_000225605.1, Zheng et al., 2011) using all the protein sequences of the ustiloxin BGC from *U. virens* (GenBank: BR001221.1, Tsukui et al., 2015) as queries. Genomes of some species of *Cordyceps* s.l., including *Cordyceps pruinose* (GCA_003025255.1), *B. bassiana* (GCA 000280675.1), *B. brongniartii* (GCA_001636735.1), *C. chanhua* (GCA_002968875.1), *C. fumosorosea* (GCA_001636725.1), *Cordyceps tenuipes* (GCA_003025305.1), *M. robertsii* (GCA_000591435.1), and *O. sinensis* (GCA_012934285.1) were downloaded from GenBank and BLASTP searches were performed against these genomes using the ustiloxin BGC from *C. militaris* as queries.

2.3. Gene deletion and complement by AMA1-based CRISPR/Cas9 system

CmustYa and *CmustYb* were knocked out simultaneously by a single sgRNA with donor DNAs. The 20 bp sgRNA that flanked a protospacer adjacent motif sequence for gene deletion was obtained from the nucleotide sequence of the intergenic region between *CmustYa* and *CmustYb* using an online eukaryotic pathogen CRISPR guide RNA/DNA Design Tool (Peng & Tarleton, 2015). The sgRNA expression cassette CmtRNApro-sgRNA1-T6 was introduced into the pAMA1-Cas9 plasmid (Meng et al., 2022) at the *Bst*EII loci to construct the plasmid pAMA1--Cas9-sgRNAc$_{mustYaYb}$. The HDR templates (donor DNAs) of the targeted loci were amplified from *C. militaris* using primers Up1-F/R and Down1-F/R from the flanking sequences of *CmustYb* and *CmustYa*, respectively. The purified PCR fragments were then cloned into pAMA1-Cas9-sgRNA$_{CmustYaYb}$ to construct the plasmid for deletion, pAMA1-Cas9-sgRNA$_{CmustYaYb\text{-HR}}$.

CmustYa and *CmustYb* were complemented *in-situ* by a single sgRNA with donor DNAs. The sgRNA expression cassette CmtRNApro-sgRNA2-T6 was introduced into the pAMA1-Cas9 plasmid (Meng et al., 2022) to construct the plasmid pAMA1-Cas9-sgRNA$_{CmustYaYb\text{-COM}}$. The HDR templates including left and right arms of the HDR template used in deletion, the whole sequence of *CmustYb*, *CmustYa* and the intergenic region were

amplified from *C. militaris* WT strain using primers Up1-F/Down1-R. The purified PCR fragments were then cloned into pAMA1-Cas9-sgRNAc$_{CmustYaYb\text{-com}}$ to construct the plasmid for complementation, pAMA1-Cas9-sgRNA$_{CmustYaYb\text{-com-HR}}$. Then, deletion and complementation plasmids were introduced into the WT and deletion strains, respectively according to our previously described procedures (Meng et al., 2022). Mutant strains obtained were verified by PCR with primers Up-F/Down-R and reverse transcription PCR (RT-PCR) with *CmustYb* F/R and *rpb1*F/R primers. Plasmid loss for the deletion strain was performed (Meng et al., 2022) and identified by PCR with *Hyg*R F/R primers. The deletion strain after plasmid loss was deposited in the China General Microbiological Culture Collection Center under accession number CGMCC 40266.

2.4. Off-target analyses for the deletion strain by PCR and whole-genome resequencing

Off-target analyses were performed by PCR and Sanger sequencing, and whole-genome resequencing. Putative off-target sites were identified by Cas-OFFinder v2.4 (http://www.rgenome.net/cas-offinder/, Bae et al., 2014) against the reference genome of *C. militaris* strain CM01 (Table S1). The specific primers that surrounded the putative off-target sites were designed and used to perform PCR amplification (Table S2), the *ΔCmustYb-CmustYa* strain (CGMCC 40266) was used for off-target analysis. The products were sequenced using the Sanger method. Genomic DNA of the deletion strain CGMCC 40266 was extracted via the CTAB method and then subjected to whole-genome resequencing on the MGI sequencing platform (Nextomics Biosciences Co., Ltd., Wuhan, China). Clean data (4G) were obtained after quality control and deposited in GenBank under accession number PRJNA970099. The re-sequencing data were aligned to the genome potential off-target sites, knockout gene sequence, and plasmid sequence using BWA v0.7.15 (Li & Durbin, 2009).

2.5. Phylogeny of selected Cordyceps sensu lato species

The ITS sequences obtained from GenBank for selected *Cordyceps* sensu lato species were used for phylogenetic analyses (Table S3). Each sequence was extracted and aligned using MAFFT v7 with default parameters (Katoh & Standley, 2013). Maximum Likelihood (ML) tree was searched using RAxML v8 (Stamatakis, 2014) with 1000 bootstrap replicates.

2.6. Statistical analysis

All statistical analyses were performed using SPSS software version 25.0 (IBM Corp., Armonk, NY, USA). Data were shown as means ± SD of three technical replicates. For multi-group comparison, P values were derived from one-way ANOVA. For two-group comparison, P values were derived from the one-way Student's *t*-test to determine differences between groups with normally distributed data. One, double and triple asterisks represented significant differences at $P < 0.05$, $P < 0.01$ and $P < 0.001$, respectively. P-value of less than 0.05 was considered statistically significant. Graphical representations of the data were created using GraphPad Prism version 8.0 (GraphPad Software, San Diego, CA, USA).

3. Results and discussion

3.1. Prediction of a RiPP cluster associated with ustiloxins in Cordyceps militaris genome

Though *Cordyceps* fungi such as *C. militaris* and *C. chanhua* have been used as both traditional medicines and novel foods, most BGCs have not been analyzed and safety concerns associated the consumptions of these unique fungi are still being debated as the possibility of mycotoxin production has not yet been systematically investigated (Chen et al., 2020). Fungal RiPP has initially been detected in 2007 (Hallen et al., 2007), and this group of natural products has undergone rapid expansion since then. Ustiloxins are representative RiPPs within the dikaritins (Hallen et al., 2007) and are cyclopeptide mycotoxins that have been confirmed to be produced by *U. virens* (Koiso et al., 1992) and *A. flavus* (Tsukui et al., 2015).

Three genes (*CCM_02059*, *02060*, and *02061*) of the RiPP cluster in the *C. militaris* genome were reported to exhibit some sequence similarity with *AFLA_094990* and *AFLA_094960* in the *A. flavus* gene cluster, which has been confirmed to be responsible for the biosynthesis of ustiloxin B (Zhang et al., 2022). However, there were great differences in the gene order and direction between these two clusters. Further analysis revealed that the genes of the RiPP cluster in *C. militaris* genome showed higher sequence similarities (Table S4) with the genes of ustiloxin BGC in *U. virens* (Tsukui et al., 2015), with an almost identical gene order and direction (Fig. S1), except that the *U. virens* cluster lacks a homolog of *CCM_02065*, which is the *C. militaris* homolog of *ustH* in *A. flavus* ustiloxin BGC (Umemura et al., 2014). The genes, *CCM_02058*, *CCM_02059* and *CCM_02060* encoded three oxidases essential for cyclization of the core peptide and were orthologous to *UvustQ*, *UvustYb* and *UvustYa*, respectively (Fig. S1, Table S4). Accordingly, we named the *C. militaris* orthologs as *CmustQ*, *CmustYb* and *CmustYa*, respectively. Whether this predicted *RiPP* cluster was responsible for ustiloxin production in *C. militaris* is indeed critical for this edible mushroom.

3.2. Gene transcript levels of the putative ustiloxin BGC in Cordyceps militaris

Gene expressions of the putative ustiloxin BGC were profiled using the transcriptomics data across different developmental stages, including mycelia, early sclerotium, late sclerotium, primordium and mature fruiting body, of *C. militaris* (GenBank PRJNA972643). All the genes in the putative ustiloxin BGC exhibited similar transcript regulation across the sampled stages. Namely, all the BGC genes expressed at a pretty low level at the mycelial stage and the highest level at the stage of late sclerotium (Fig 1A). At the stages of primordium and mature fruiting body, the transcript levels decreased but were still much higher than those of the mycelial stage (Fig 1A). The RNA levels were verified with qPCR analysis (Fig 1B). Especially, the gene encoding for the precursor peptide, *CmustA*, showed the most up-regulation at the stages of early and late sclerotium.

3.3. Predicted ustiloxins produced by Cordyceps militaris based on the precursor peptide

Ustiloxin synthesis begins with the precursor peptide, which is encoded by *UstA* in *A. flavus* (Umemura et al., 2014). The gene *CmustA* was cloned using the DNA of *C. militaris*

strain CGMCC 3.16320, and the sequence has been deposited in the NCBI under the accession number OP700048. The protein CmUSTA was predicted with a signal peptide, a core peptide, and a C-terminal recognition sequence which was consistent with other RiPPs precursor peptides (Umemura et al., 2014).

As for the core peptide, the predicted CmUSTA possesses 19-fold sequence repeats, of which four contain a YAIG (Tyr-Ala-Ile-Gly) motif, 13 contain a YAIA (Tyr-Ala-Ile-Ala) motif, and two contain a YVIP (Tyr-Val-Ile-Pro) motif (Fig. 2A). The ustiloxin precursor peptide contain the core peptides YVIG and YAIG for ustiloxins A and B, respectively in *U. virens*, whereas that of *A. flavus* only equips with the YAIG motif for ustiloxin B. Correspondingly, *U. virens* produces ustiloxins A and B, whereas *A. flavus* only synthesizes ustiloxin B (Tsukui et al., 2015). According to amino acids sequences of the precursor peptides, it was predicted that *C. militaris* might produce ustiloxin B and two kinds of new ustiloxins (Fig. 2B), and that it was likely not produce any ustiloxin A.

3.4. Confirmation of ustiloxin B and a new ustiloxin produced by Cordyceps militaris

The fruiting bodies of *C. militaris* cultivated on wheat and pupae of *Antheraea pernyi* were pretreated using polymer cation exchange cleanup followed by HPLC analysis separately. Two compounds, with retention time at 20 min (compound 1) and 22 min (compound 2), were identified in the HPLC-UV profile (Fig 3A) in both samples. In order to rule out the possibility that the compounds were residuals from cultivation substrates, the pupae of *A. pernyi* and wheat samples were pretreated and tested with the same approach. No peak was detected at the corresponding retention time (Fig. 3A). Therefore, the compounds 1 and 2 were produced by *C. militaris* rather than the residuals from the cultivation substrates.

The compound 1 was determined to possess a molecular formula $C_{26}H_{39}N_5O_{12}S$ with a mass of 646.2380 [M + H] + by mass spectrum (Fig. S2A) and a structure same as the known ustiloxin B characterized by chemical shifts in ^{1}H NMR spectroscopy (Table S5) (Shan et al., 2012). Four repeats of YAIG in the core peptide of CmUSTA (Fig. 2A) were consistent with the fact that *C. militaris* can produce ustiloxin B. However, the [M + H] + ion peak of the compound 2 did not match any known ustiloxins, indicating that it may be an unknown ustiloxin analogue (Fig. S2B). The compound 2 was isolated as a white amorphous solid by semi-preparative HPLC and molecular formula was determined as $C_{27}H_{41}N_5O_{12}S$ with a mass of 658.2483 ($[M - H]^-$) and 660.2545 ($[M - H]^+$) (Fig. S2B). It had 14 mass units more than ustiloxin B, suggesting that it may have one more methyl group, which was further verified by UPLC-MS/MS analysis (Fig. 3B). The ion fragments of m/z 185 and 179 were consistent with the reported of ustiloxin B and m/z 88 was assumed to be the substitution of alanine for glycine in the compound 2. The ion fragments of m/z 330, 465, 479 and 640 were supposed to carry a methyl substituent at C19 (Fig. 3C). To further assess the structure of compound 2, NMR was carried out. The characteristic ^{1}H NMR signal of the proton at C19 was a quartet at δH 4.16 (q, J=7.3 Hz, 1H), instead of the doublet at 3.67 (d, J= 17.2, 1H) and 3.73 (d, J= 17.2, 1H) observed in ustiloxin B (Table S5). In addition, a doublet at 1.35 (d, J= 7.3 Hz, 3H), which could not be observed in ustiloxin B, suggested a methyl substitution at C19. Furthermore, the substitution pattern on C19 was established by ^{13}C NMR and ^{1}H—^{1}H COSY experiments. The ^{13}C NMR spectra of the

compound 2 lacked the signal assigned for the C19 at δC 44.2 of ustiloxin B (Koiso et al., 1992), and instead exhibited signals at δC 49 and 15 which were similar to chemical shift of C6 and C24 (Fig . 3C). The presence of two CH—CH_3 moiety in the compound 2 was verified by ^{3}H—^{3}H COSY (Fig. S2C). Thus, the compound 2 was determined as a methyl substituent at C19 of ustiloxin B, resulted in the substitution of glycine of ustiloxin B by alanine moiety (Fig. 3B). The structure was consistent with the prediction based on the core peptide of CmUSTA (YVIA). Eight types of ustiloxins, comprising ustiloxins A to H, have been discovered in rice false smut balls (Koiso et al., 1994, 1998; Wang et al., 2017; Ye et al., 2016). As a result, this newly discovered ustiloxin was designated as ustiloxin I. For ustiloxins, the CH_3NH, phenolic hydroxy, and alkyl substituents at the C2 and C6 positions are important for inhibiting microtubule assembly (Zhang et al., 2023). These functional groups were all retained in the structure of ustiloxin I, indicating its similar bioactivity as ustiloxin B. However, the predicted third ustiloxin in *C. militaris* was not detected with the same approaches, and this could be explained with the extremely low quantity due to its' only two repeats (YVIP).

In addition, seven *C. militaris* fruiting body materials were sampled from various markets in China, including *Cordyceps* markets in Yunnan, Shandong, Liaoning, Inner Mongolia and Jiangsu provinces. The two ustiloxins were detectable in all the samples, and the content of ustiloxin I was much higher than that of ustiloxin B in those samples (Fig. S3). It was reported that in *A. flavus*, ustiloxin B production increased quadratically with increasing repeat number of YAIG inUSTA variants (Umemura et al., 2022). Therefore, the ustiloxin concentration is probably associated with the number of the repeats in the core peptide in *C. militaris*, given CmUSTA possessed four YAIG motifs as ustiloxin B, fewer than the higher number of 13-YAIA in ustiloxin I (Fig 2A).

The content of ustiloxins in fruiting bodies grown on pupae from Liaoning province was higher than other fruiting bodies grown on wheat medium. To verify whether the contents of ustiloxins in pupae fruiting bodies are always higher than those from the wheat cultures, fruiting bodies of three different strains (Dong-1, 633 and 1532) cultivated on pupae and wheat medium respectively were examined (Fig. S4). The contents of the two ustiloxins in the fruiting bodies cultivated on pupae were significantly higher ($P < 0.05$) than those cultivated on wheat medium (Fig. S5A). Regarding the contents of ustiloxin B, the pupae fruiting bodies exhibited over 2 times more than those of wheat fruiting bodies.

In fact, multiple fruiting bodies of *C. militaris* cultivated on pupae arise from a resistant structure called sclerotium, and ustiloxins contents were detected respectively from both the sclerotium and fruiting body (Fig. S5B) in the cultivated samples of the three strains mentioned above as well as two wild samples (Fig. S5B). *C. militaris* accumulated more ustiloxins in fruiting bodies than in the sclerotia for both the cultivated and wild samples (Fig. S5C).

Ustiloxin contamination in rice was nearly ubiquitous globally. According to a recent study, there are various ustiloxins in rice, among which ustiloxin A is predominant with an occurrence of 46.1% and an average concentration of 49.71 μg/kg, followed by ustiloxin B (31.1%, 13.31 μg/kg) and ustiloxin G (18.4%, 9.19 μg/kg, Hu et al., 2023). It was confirmed

that ustiloxins have become a potential danger for food security (Hu et al., 2019). Our initial findings revealed the presence of two types of ustiloxins, including ustiloxins B and I, with the content of ustiloxins in *C. militaris* being significantly higher than those found in rice. Though the daily intake of *C. militaris* is lower than that of rice, and the toxicity of ustiloxin I remains unsolved, there is certainly a need to eliminate the ustiloxins from *C. militaris* fruiting bodies, one of the popular food sources.

3.5. CRISPR/Cas9-mediated deletion and complement confirmed that the RiPP cluster is responsible for ustiloxin production in Cordyceps militaris

CRISPR/Cas9-mediated gene editing has been used for quality improvement of crops extensively. An AMA1-based CRISPR/Cas9 system for highly efficient marker-free gene editing and a precisely targeted gene deletion via HDR was constructed in *C. militaris* by this team (Meng et al., 2022), paving the way to its application in the engineering with this edible fungus.

The genes, *CmustYb* (*CCM_02059*) and *CmustYa* (*CCM_02060*) contain the same conserved domain DUF3328 (UstYa homolog) and both encode oxidases, which are essential for the cyclization of the core peptide in biosynthesis of ustiloxins. In *A. flavus*, the deletion mutants of *AFLA_094990* (*ustYa*) resulted in the loss of ability to synthesize ustiloxin B completely, while the deletion mutants of *AFLA_095020* (*ustYb*) still produced a small amount of ustiloxin B (Umemura et al., 2014). To verify the prediction that this gene cluster is responsible for ustiloxins biosynthesis in *C. militaris*, and most importantly, to obtain *C. militaris* strain producing no ustiloxins, two adjacent genes, *CmustYb* and *CmustYa*, were precisely removed using our well-established CRISPR/Cas9 system based on autonomously replicating plasmid with an AMA1 sequence with donor DNAs (Meng et al., 2022).

CmustYb and *CmustYa* are 934 bp and 730 bp in length, respectively. There are 647 bp for the intergenic region (Fig. 4A), in which the sgRNA was designed. DNA fragments of 507 bp for the left arm flanking the target gene of *CmustYb* and 643 bp for the right arm flanking *CmustYa* were cloned and used as HDR templates (Fig. 4A). The pAMA1-Cas9-sgRNA$_{CmustYaYb\text{-HR}}$ containing sgRNA and HDR templates was transferred to *C. militaris* by polyethylene glycol-mediated protoplast transformation. *CmustYb-CmustYa* fragment (2307 bp) was completely deleted (Fig. 4B) and the transformants displayed the anticipative length of a band at 1197 bp with primer Up-F/Down-R (Fig. 4C). The RT-PCR results revealed that *CmustYb-CmustYa* of the knockout transformant was transcriptionally inactive (Fig. 4C). Therefore, the two adjacent core genes, *CmustYb* and *CmustYa*, were deleted precisely and simultaneously by a single sgRNA designed in the intergenic region using CRISPR/Cas9 system. It was demonstrated that this strategy is more effective since multiple gene editing using several sgRNAs is laborious with a low efficiency.

Next, plasmid loss was performed by picking the single clone with toothpicks and subculture. After the subculture of knockout transformant, no conidia germination was observed on selective plates with hygromycin, whereas mycelia appeared on nonselective plates (Fig. S6A), indicating that the pAMA1-Cas9-sgRNA$_{CmustYaYb\text{-HR}}$ with the AMA1 sequence was lost. Furthermore, *hyg* sequence cannot be amplified with primer *hyg* F/R

while ITS sequence could be detected with ITS4/5, confirming the loss of the pAMA1-Cas9-sgRNA$_{CmustYaYb\text{-HR}}$ (Fig. S6B). The deletion strain after plasmid loss was used for the further experiments.

CmustYb and *CmustYa* were complemented *in-situ* by the same CRISPR/Cas9 system. The sgRNA2 was designed in the sequence of HDR template used in the deletion (Fig. 4A). The plasmids with sgRNA expression cassette and complementation donors were transformed to the *ΔCmustYb-CmustYa* strain and *in-situ* complementation strains of above two genes were obtained (Fig. 4C).

As expected, the deletion of *CmustYb* and *CmustYa* resulted in a complete loss of ustiloxin production in the fruiting bodies and ustiloxins were successfully detected in those cultivated with the *in-situ* complementation strain by HPLC analyses (Fig. S7), confirming that this RiPP gene cluster is responsible for ustiloxin production in *C. militaris*.

Unlike in model fungi such as *Neurospora crassa* and *Aspergillus niger*, the genetic manipulation in macrofungi like *Cordyceps* can be challenging and often with a low efficiency. Here, by the CRISPR/Cas9 system, the first gene complement *in-situ* was fulfilled in *C. militaris*. Actually, the phenotype of ustiloxin production cannot be recovered in the *ex-situ* complement strain (Fig. S7). Deletion and *in-situ* complement of the two core genes confirmed that this BGC was responsible for the production of ustiloxin, most importantly, a ustiloxin-free *C. militaris* strain was generated.

3.6. CRISPR/Cas9-mediated deletion of CmustYb and CmustYa exhibited no obvious effects on the growth and development of Cordyceps militaris

There was no significant difference in the growth rates between the WT and *ΔCmustYb-CmustYa* strains that were incubated at 21 °C. No obvious difference in colony color was observed when all the strains were cultured on PDA plates after being irradiated for 4 d (Fig. 5A). The WT and *ΔCmustYb-CmustYa* strains were grown to induce the formation of fruiting bodies, and it was found that the *CmustYb* and *CmustYa* deletion did not impair the development of fruiting bodies of the fungus on both wheat medium and pupae of *A. pernyi*. The fruiting bodies of the mutant were neat and uniform with bright color, and the yield in the mutant was as high as the WT strain (Fig. 5B).

The stability of continuous subculture of strains was considered as a critical factor in the *Cordyceps* industry. The mutant and WT strains were subcultured for seven consecutive passages and used for the fruiting body cultivation, respectively. The biological efficiency and the phenotypes of the third, fifth and seventh passages exhibited no detectable differences between the strains. Namely, the fruiting bodies of both the mutant and WT strains were in the similar shades of yellow. The fruiting body sizes were almost uniform except for a little deform for the seventh mutant strain (Fig. 5C). All of these indicated that the agronomic traits of deletion strains were effectively maintained.

3.7. No off-target sites and foreign sequences were identified by PCR and genome resequencing

The application of CRISPR/Cas9 systems in breeding may be hindered by off-target and foreign gene insertion. In the recent studies with *Pleurotus ostreatus* (Koshi et al., 2022) and *Ceriporiopsis subvermispora* (Nakazawa et al., 2022), part of the plasmid fragment and *cas9* sequence had been integrated into the target site. The off-target events and foreign gene insertion were detected by both PCR and genome resequencing.

Among the 37 predicted off-target sites, the top 4 scoring loci were selected where all have three mismatches in the twenty nucleotides upstream the NGG PAM sequence (Table S1). After PCR and sequencing, no mutations were found around the putative off-target sites in the edited strain (Fig. S8). These results demonstrated that the sgRNA had a high specificity for targeting the *CmustYb* and *CmustYa* genes in *C. militaris*. Then, genome of the deletion strain was re-sequenced and analyzed. By comparison between the genomes of the deletion and WT strains, it was found that there were no base mutations, insertions, or deletions in all the 37 predicted off-target sites and their surrounding sequences. Furthermore, the sequences of deleted genes and the used plasmid (including *Cas9*, AMA1 and *HygR* etc.) were not presented in the edited strain by blast analysis. Consistent with our previous research (Liu et al., 2023), there was no residual of foreign sequences, suggesting the advantage of extrachromosomal replication of AMA1 plasmid without integration into the host genome. This ustiloxin-free strain, developed via the AMA1-based CRISPR/Cas9 system, will be expected to have extensive application prospects.

3.8. Ustiloxin BGC in the genomes of Cordyceps s.l. and ustiLoxin production

Genome surveys revealed that the homologous ustiloxin BGC of *C. militaris* was also presented in the genomes of some species of *Cordyceps* sensu lato, including *C. pruinosa*, *C. fumosorosea*, *C. chanhua* and *C. tenuipes*. There was a conserved cluster synteny of the ustiloxin BGCs among the genomes of these five *Cordyceps* species and over 60% sequence identity for all the genes among the four species being compared with the corresponding gene of the *C. militaris* BGC (Fig. 6A).

The precursor peptide sequences of the above *Cordyceps* species all contained N-terminal signal peptides and similar USTA and repeat sequences. The multiple repeat sequences possess "YAIG" as the core peptide, and no "YVIG" sequence was observed (Fig. S9), indicating that these species can produce ustiloxin B but not ustiloxin A. “YAIA” repeats are specific in the core peptide of the tested *Cordyceps* species, indicating these *Cordyceps* species maybe also capable to produce the new ustiloxin I, suggesting that ustiloxin I is likely *Cordyceps* specific.

Further the presence of such a BGC were examined in other Sordariomycetes species that are closely related to *Cordyceps*, including *B. bassiana*, *B. brongniartii*, *M. robertsii* and *O. sinensis*, to assess possible changes of the BGC components along the evolution of *Cordyceps* fungi. No complete set of ustiloxin BGC was observed in the selected genomes of *Beauveria*, *Metarhizium* and *Ophiocordyceps* species, except a few BGC genes that were conserved in sequence and gene synteny between these genomes and *Cordyceps* genomes

(Fig. 6B). Whether these fungi are capable of producing fully functional ustiloxins requires a further investigation.

Fruiting body tissues or mycelia (only *M. robertsii*) of different *Cordyceps* sensu lato species were also sampled (Fig. 6C) and the water extracts were analyzed by HPLC to verify whether they can produce ustiloxins. As expected, two types of ustiloxins were detected from cultured *C. fumosorosea*, *C. tenupies* and *C. chanhua* (Fig. 6D), confirming that the homolog BGCs of these species were responsible for ustiloxin synthesis. So far, ustiloxins A-H have been identified from rice false smut balls, with ustiloxin A being the primary and most toxic component. Our data further confirmed that *Cordyceps* species were unable to produce ustiloxin A. It was also indicated that there were some differences between the ustiloxin produced in *Cordyceps* and those produced in *U. virens*.

Ustiloxins exhibited various bioactivities, including antimitotic behaviors by inhibiting microtubule assembly and skeleton formation of the eukaryotic cells and are regarded as potential antitumor agents for clinical applications (Wang et al., 2016). Our ongoing projects are focused on exploring the toxicity and potential applications of *Cordyceps* specific ustiloxin I as medicinal and agrochemical agents. For the species of *C. chanhua*, a novel food approved by Chinese government, and *C. tenuipes*, which is being utilized in a variety of functional foods in Japan and South Korea (Dong et al., 2022), ustiloxins should be a concern in the future. For the phylogenetically related species *B. bassiana*, *B. brongniartii*, *M. robertsii* and *O. sinensis*, there were no complete ustiloxin BGCs in the genome (Fig. 6B) and no ustiloxins were detected (Fig. 6D). The evolution of ustiloxin BGC in the *Cordyceps* s.l. May have undergone repeat losses and/or gains (Fig. 6B).

4. Conclusions

In this study, a RiPP cluster was demonstrated to be responsible for ustiloxin production in *C. militaris*. Ustiloxin B and a novel ustiloxin I were identified and characterized through extraction and structural analysis. By employing CRISPR/Cas9 technology, the core genes *CmustYb* and *CmustYa* were deleted. This deletion led to the development of a strain of ustiloxin-free that exhibited comparable agronomic traits to those of the wild type strain during fruiting body cultivation. Importantly, PCR and genome resequencing confirmed the absence of off-target events or foreign sequence remnants in the ustiloxin-free strain. This elimination of ustiloxin production ensures the safe use of *C. militaris* as food or alternative medicine. Ustiloxins B and I were also detected in some *Cordyceps* species, such as *C. fumosorosea*, *C. chanhua* and *C. tenuipes*, but not in other phylogenetically related species, suggesting repeat losses and/or gains of ustiloxin BGC during evolution. Overall, this report underscores the potential of CRISPR technology in enhancing food safety by controlling ustiloxins in *C. militaris*, with broader implications for improving food quality.

Supplementary Material

Refer to Web version on PubMed Central for supplementary material.

Acknowledgment

This work was supported by grants from the National Key Research and Development Program of China project [2022YFD1200602]; Science and Technology Cooperation Project of Chifeng Regional Collaborative Innovation Platform [2022zk007]; the National Institutes of Health R01 grant [AI146584]; and the National Science Foundation grant [IOS 1457044].

We are grateful to Prof. Gang Liu from Institute of Microbiology, Chinese Academy of Sciences for supporting with the establishment AMA1-based CRISPR/Cas9 system and Prof. Yang Liu from Huazhong Agricultural University for isolation and identification of ustiloxin. We thank Prof. Chengshu Wang from Institute of Plant Physiology and Ecology, Chinese Academy of Science and Hong Yu from Yunnan University for providing strain *Metarhizium robertsii* strain ARSF23 and *Cordyceps fumosorosea* strain. We very appreciate Dr. Baosong Chen, Wenzhao Wang, Erwei Li and Jinwei Ren from the Institute of Microbiology, Chinese Academy of Sciences for the help with the MS and NMR analyses. We also thank the anonymous reviewers and editors for their helpful comments and suggestions.

Data availability

Data will be made available on request.

References

Bae S, Park J, & Kim JS (2014). Cas-OFFinder: A fast and versatile algorithm that searches for potential off-target sites of Cas9 RNA-guided endonucleases. Bioinformatics, 30, 1473–1475. 10.1093/bioinformatics/btu048 [PubMed: 24463181]

Barrangou R, & Doudna JA (2016). Applications of CRISPR technologies in research and beyond. Nature Biotechnology, 34, 933–941. 10.1038/nbt.3659

Blin K, Shaw S, Kloosterman AM, Charlop-Powers Z, Van Wezel GP, Medema MH, & Weber T (2021). antiSMASH 6.0: improving cluster detection and comparison capabilities. Nucleic Acids Research, 49, 29–35. 10.1093/nar/gkab335

Chen B, Sun Y, Luo F, & Wang C (2020). Bioactive metabolites and potential mycotoxins produced by *Cordyceps* fungi: A review of safety. Toxins, 12, 410. 10.3390/toxins12060410 [PubMed: 32575649]

Cunningham KG, Manson W, Spring FS, & Hutchinson SA (1950). Cordycepin, a metabolic product isolated from cultures of *Cordyceps militaris* (Linn.) Link. Nature, 166, 949. 10.1038/166949a0

Dong QY, Wang Y, Wang ZQ, Tang DX, Zhao ZY, Wu HJ, & Yu H (2022). Morphology and phylogeny reveal five novel species in the genus *Cordyceps* (Cordycipitaceae, Hypocreales) from Yunnan, China. Frontiers in Microbiology, 13, Article 46909. 10.3389/fmicb.2022.846909

Dudgeon WD, Thomas DD, Dauch W, Scheett TP, & Webster MJ (2018). The effects of high and low-dose *Cordyceps militaris*-containing mushroom blend supplementation after seven and twenty-eight days. American Journal of Sports Science, 6, 1–7. 10.11648/j.ajss.20180601.11

Gao YL, Yu C, & Li L (2022). Heterologous expression of a natural product biosynthetic gene cluster from Cordyceps militaris. Journal of Antibiotics, 75, 16–20. 10.1038/s41429-021-00478-3 [PubMed: 34548637]

Hallen HE, Luo H, Scott-Craig JS, & Walton JD (2007). Gene family encoding the major toxins of lethal Amanita mushrooms. Proceedings of the National Academy of Sciences of the United States of America, 104, 19097–19101. 10.1073/pnas.0707340104 [PubMed: 18025465]

Hu Z, Dang Y, Liu C, Zhou L, & Liu H (2019). Acute exposure to ustiloxin A affects growth and development of early life zebrafish, *Danio rerio*. Chemosphere, 226, 851–857. 10.1016/j.chemosphere.2019.04.002 [PubMed: 30978596]

Hu Z, Qian S, Fan K, Yu Y, Liu X, Liu H, Meng J, Zhao Z, & Han Z (2023). Natural occurrence of ustiloxins in rice from five provinces in China and the removal efficiencies of different milling steps. Journal of the Science of Food and Agriculture. 10.1002/jsfa.12698

Jędrejko KJ, Lazur J, & Muszyńska B (2021). *Cordyceps militaris*: An overview of its chemical constituents in relation to biological activity. Foods, 10, 2634. 10.3390/foods10112634 [PubMed: 34828915]

Jhou BY, Fang WC, Chen YL, & Chen CC (2018). A 90-day subchronic toxicity study of submerged mycelial culture of *Cordyceps militaris* in rats. Toxicological Research, 7, 977–986. 10.1039/c8tx00075a

Katoh K, & Standley DM (2013). MAFFT multiple sequence alignment software version 7: Improvements in performance and usability. Molecular Biology and Evolution, 30, 772–780. 10.1093/molbev/mst010 [PubMed: 23329690]

Koiso Y, Li YIN, Iwasaki S, Hanaka K, Kobayashi T, Sonoda R, & Sato Z (1994). Ustiloxins, antimitotic cyclic peptides from false smut balls on rice panicles caused by *Ustilaginoidea virens*. Journal of Antibiotics, 47, 765–773. 10.7164/antibiotics.47.765 [PubMed: 8071121]

Koiso Y, Morisaki N, Yamashita Y, Mitsui Y, Shirai R, Hashimoto Y, & Iwasaki S (1998). Isolation and structure of an antimitotic cyclic peptide, ustiloxin F: Chemical interrelation with a homologous peptide, ustiloxin B. Journal of Antibiotics, 51, 418–422. 10.7164/antibiotics.51.418 [PubMed: 9630863]

Koiso Y, Natori M, Iwasaki S, Sato S, Sonoda R, Fujita Y, Yaegashi H, & Sato Z (1992). Ustiloxin: A phytotoxin and a mycotoxin from false smuth balls on rice panicles. Tetrahedron Letters, 33, 4157–4160. 10.1016/S0040-4039(00)74677-6

Koshi D, Ueshima H, Kawauchi M, Nakazawa T, Sakamoto M, Hirata M, & Honda Y (2022). Marker-free genome editing in the edible mushroom, *Pleurotus ostreatus*, using transient expression of genes required for CRISPR/Cas9 and for selection. Journal of Wood Science, 68, 1–8. 10.1186/s10086-022-02033-6

Li H, & Durbin R (2009). Fast and accurate short read alignment with Burrows-Wheeler transform. Bioinformatics, 25, 1754–1760. 10.1093/bioinformatics/btp324 [PubMed: 19451168]

Liu Q, Meng GL, Wang M, Li X, Liu MQ, Wang F, Yang Y, & Dong CH (2023). Safe-harbor-targeted CRISPR/Cas9 system and *Cmhyd1* overexpression enhances disease resistance in *Cordyceps militaris*. Journal of Agricultural and Food Chemistry, 71, 15249–15260. 10.1021/acs.jafc.3c05131 [PubMed: 37807760]

Meng GL, Wang XP, Liu MQ, Wang F, Liu Q, & Dong CH (2022). Efficient CRISPR/Cas9 system based on autonomously replicating plasmid with an AMA1 sequence and precisely targeted gene deletion in the edible fungus, Cordyceps militaris. Microbial Biotechnology, 15, 2594–2606. 10.1111/1751-7915.14107 [PubMed: 35829671]

Nakazawa T, Inoue C, Nguyen DX, Kawauchi M, Sakamoto M, & Honda Y (2022). CRISPR/Cas9 using a transient transformation system in *Ceriporiopsis subvermispora*. Applied Microbiology and Biotechnology, 106, 5575–5585. 10.1007/s00253-022-12095-7 [PubMed: 35902408]

Peng D, & Tarleton R (2015). EuPaGDT: A web tool tailored to design CRISPR guide RNAs for eukaryotic pathogens. Microbial Genomics, 1, Article e000033. 10.1099/mgen.0.000033 [PubMed: 28348817]

Shan T, Sun W, Liu H, Gao S, Lu S, Wang M, & Zhou L (2012). Determination and analysis of ustiloxins A and B by LC-ESI-MS and HPLC in false smut balls of rice. International Journal of Molecular Sciences, 13, 11275–11287. 10.3390/ijms130911275 [PubMed: 23109852]

Song S, Liu X, Wei S, Liu X, & Yao L (2018). Toxicity studies of *Cordyceps militaris* in mice. Natural Product Research and Development, 30, 1878–1883. 10.16333/j.1001-6880.2018.11.005 (in Chinese).

Stamatakis A. (2014). RAxML version 8: A tool for phylogenetic analysis and post-analysis of large phylogenies. Bioinformatics, 30, 1312–1313. 10.1093/bioinformatics/btu033 [PubMed: 24451623]

Tsukui T, Nagano N, Umemura M, Kumagai T, Terai G, Machida M, & Asai K (2015). Ustiloxins, fungal cyclic peptides, are ribosomally synthesized in *Ustilaginoidea virens*. Bioinformatics, 31, 981–985. 10.1093/bioinformatics/btu753 [PubMed: 25414363]

Umemura M, Kuriiwa K, & Dao LV (2022). Tandem repeats in precursor protein stabilize transcript levels and production levels of the fungal ribosomally synthesized and post-translationally modified peptide ustiloxin B. Fungal Genetics and Biology, 60, Article 03691. 10.1016/j.fgb.2022.103691

Umemura M, Nagano N, Koike H, Kawano J, Ishii T, Miyamura Y, Kikuchi M, Tamano K, Yu J, Shin-ya K, & Machida M (2014). Characterization of the biosynthetic gene cluster for the

ribosomally synthesized cyclic peptide ustiloxin B in *Aspergillus flavus*. Fungal Genetics and Biology, 68, 23–30. 10.1016/j.fgb.2014.04.011 [PubMed: 24841822]

Wang XH, Fu XX, Lin FK, Sun WB, Meng JJ, Wang AL, Lai DW, Zhou LG, & Liu Y (2016). The contents of ustiloxins A and B along with their distribution in rice false smut balls. Toxins, 8, 262. 10.3390/toxins8090262 [PubMed: 27608042]

Wang X, Gao YL, Zhang ML, Zhang HD, Huang JZ, & Li L (2020). Genome mining and biosynthesis of the acyl-CoA: Cholesterol acyltransferase inhibitor beauveriolide I and III in *Cordyceps militaris*. Journal of Biotechnology, 75, 16–20. 10.1016/j.jbiotec.2020.01.002

Wang XH, Wang J, Lai DW, Wang WX, Dai JG, Zhou LG, & Liu Y (2017). Ustiloxin G, a new cyclopeptide cycotoxin from rice false smut balls. Toxins, 9, 54. 10.3390/toxins9020054 [PubMed: 28208606]

Yan XT, Bao HY, & Bau T (2010). Isolation and identification of one natural pigment from cultured *Cordyceps militaris*. Mycosystema, 29, 777–781. 10.13346/j.mycosystema.2010.05.018 (in Chinese).

Ye Y, Minami A, Igarashi Y, Izumikawa M, Umemura M, Nagano N, Machida M, Kawahara T, Shin-Ya K, Gomi K, & Oikawa H (2016). Unveiling the biosynthetic pathway of the ribosomally synthesized and post-translationally modified peptide ustiloxin B in filamentous fungi. Angewandte Chemie International Edition, 55, 8072–8075. 10.1002/anie.201602611 [PubMed: 27166860]

Zhang JJ, Wang F, Liu MQ, Fu MJ, & Dong CH (2022). Dynamic genome-wide transcription profiling and direct target genes of CmWC-1 reveal hierarchical light signal transduction in *Cordyceps militaris*. Journal of Fungi, 8, 624. 10.3390/jof8060624 [PubMed: 35736107]

Zhang JJ, Wang F, Liu KB, Liu Q, Yang Y, & Dong CH (2018). Heat and light stresses affect metabolite production in the fruit body of the medicinal mushroom *Cordyceps militaris*. Applied Microbiology and Biotechnology, 102, 4523–4533. 10.1007/s00253-018-8899-3 [PubMed: 29594343]

Zhang JX, Wen CT, Duan YQ, Zhang HH, & Ma HL (2019). Advance in *Cordyceps militaris* (linn) link polysaccharides: Isolation, structure, and bioactivities: A review. International Journal of Biological Macromolecules, 132, 906–914. 10.1016/j.ijbiomac.2019.04.020 [PubMed: 30954592]

Zhang Y, Xu Q, Sun Q, Kong R, Liu H, Yi X, Liang Z, Letcher RJ, & Liu C (2023). Ustiloxin A inhibits proliferation of renal tubular epithelial cells in vitro and induces renal injury in mice by disrupting structure and respiratory function of mitochondria. Journal of Hazardous Materials, 448, Article 130791. 10.1016/j.jhazmat.2023.130791 [PubMed: 36706486]

Zheng P, Xia Y, Xiao GH, Xiong CH, Hu X, Zhang SW, Zheng HJ, Huang Y, Zhou Y, Wang SY, Zhao PG, Liu XZ, Leger RJS, & Wang CS (2011). Genome sequence of the insect pathogenic fungus *Cordyceps militaris*, a valued traditional Chinese medicine. Genome Biology, 12, R116. 10.1186/gb-2011-12-11-r116 [PubMed: 22112802]

Ministry of Health of the People's Republic of China. (2009). Announcement on approval of Cordyceps militaris as a novel food. Retrieved from http://www.moh.gov.cn/publicfiles/business/htmlfiles/zwgkzt/pgg/200903/39591.htm/. (Accessed 24 June 2024).

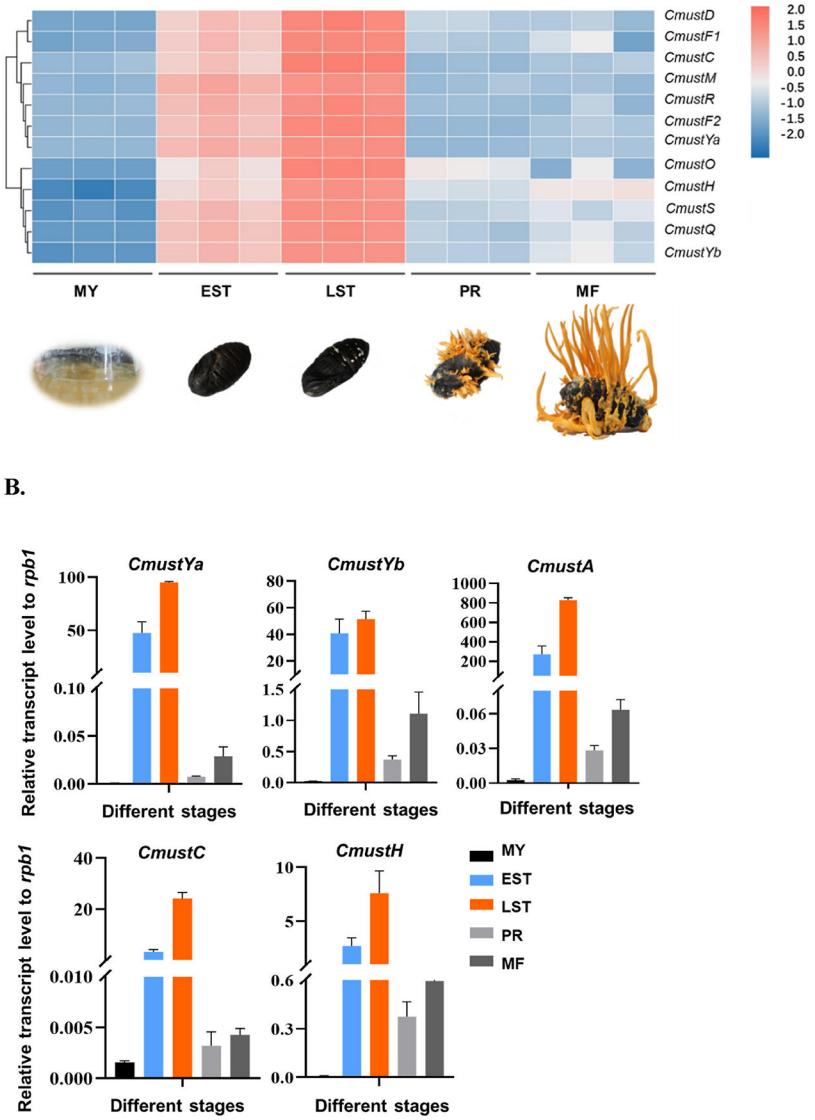

Fig. 1.

The transcript level of ustiloxin biosynthetic genes at different developmental stages (A) Samples and heat map showing the transcript level obtained from the transcriptomics data. MY: mycelium; EST: early sclerotium; LST: late sclerotium; PR: primordium; MF: mature fruiting body. (B) Transcript levels revealed by qPCR analysis. Error bars indicated the SDs of three biological replicates with three technical replicates. *Rpb1* was used as a reference gene.

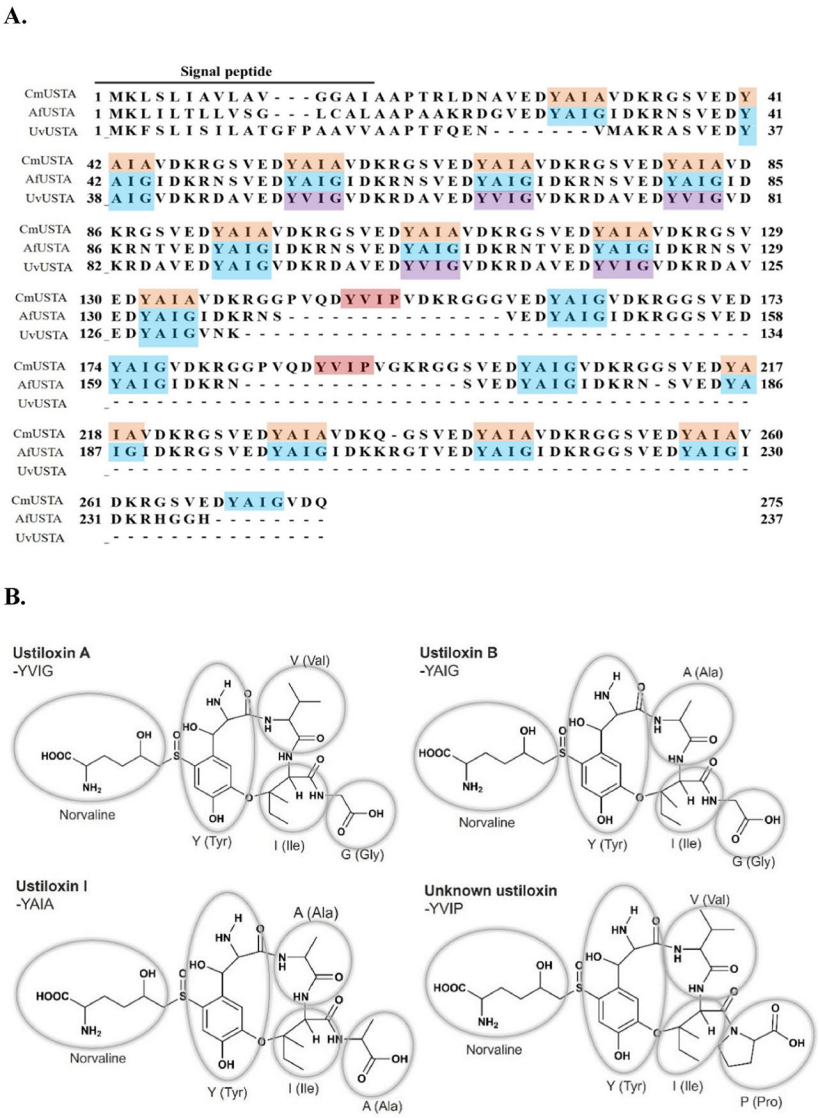

Fig. 2.

Precursor peptide sequences and prediction of ustiloxins in *Cordyceps militaris* (A) Sequence alignment of precursor peptide; CmUSTA: *C. militaris*; AfUSTA: *A. flavus*; UvUSTA: *U. virens*; YAIG, YAIA and YVIP repeats were marked in blue, orange and red, respectively. (B) Structures of ustiloxins A, B and the prediction of the new ustiloxins.

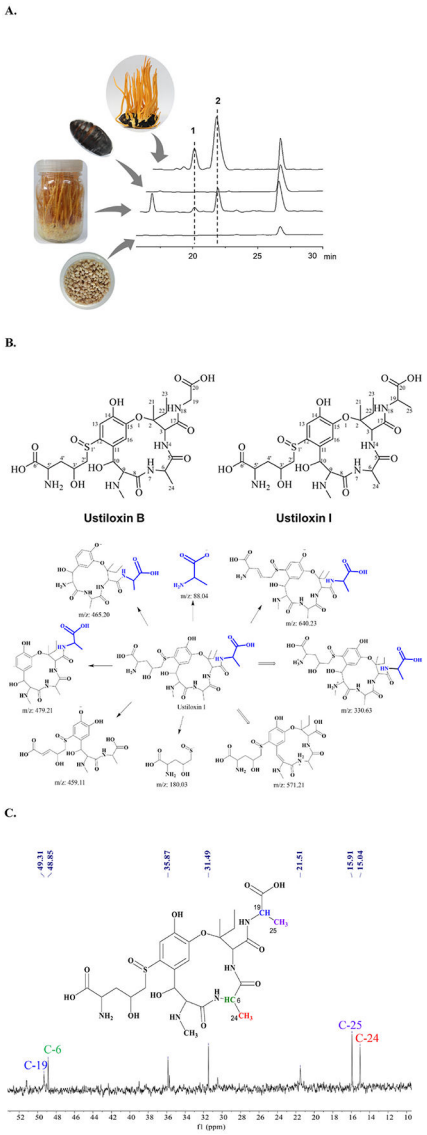

Fig. 3.

Identification of ustiloxin B and the structure analyses of a new ustiloxin in *Cordyceps militaris* (A) HPLC spectrum of the water extract of fruiting body of *C. militaris* cultivated on wheat medium and *A. pernyi*. The samples from top to bottom are fruiting bodies on *A. pernyi*, uninoculated *A. pernyi*, fruiting bodies on wheat medium and uninoculated wheat medium. (B) Structures of ustiloxins B, I and the ion fragments of the compound 2 detected by UPLC-MS/MS. (C) The signals of the substitution pattern at C19 by ^{13}C NMR.

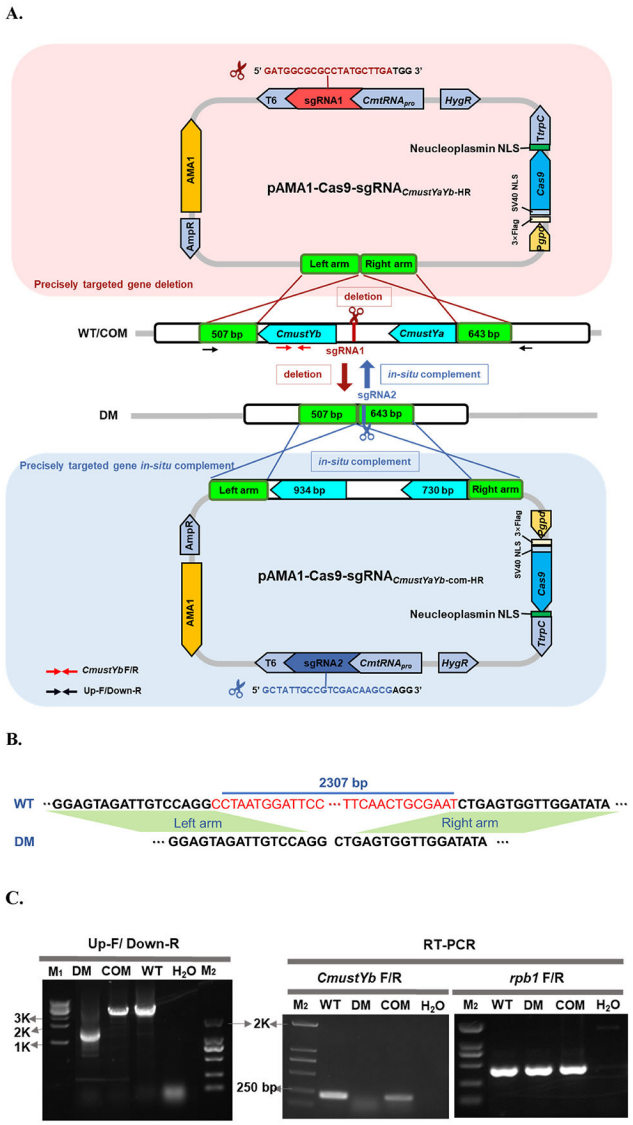

Fig. 4.

Generation and identification of the *CmustYb-CmustYa* deletion and complementation mutants in *C. militaris* by CRISPR/Cas9 (A) Strategy for the generation of *ΔCmustYb-CmustYa* and complement strain *ΔCmustYb-CmustYa::CmustYb-CmustYa* via CRISPR/Cas9-mediated homologous recombination. The sgRNA1 was designed for knockout and sgRNA2 was for complement. The left and right arms were donor templates. (B) Sanger-sequence verification of *ΔCmustYb-CmustYa*. (C) PCR and RT-PCR verification of *ΔCmustYb-CmustYa* and complement strain *ΔCmustYb-CmustYa::CmustYb-CmustYa*. WT was *C. militaris* strain CGMCC 3.16320; DM was *ΔCmustYb-CmustYa* strain; COM represented *in-situ* complementation.

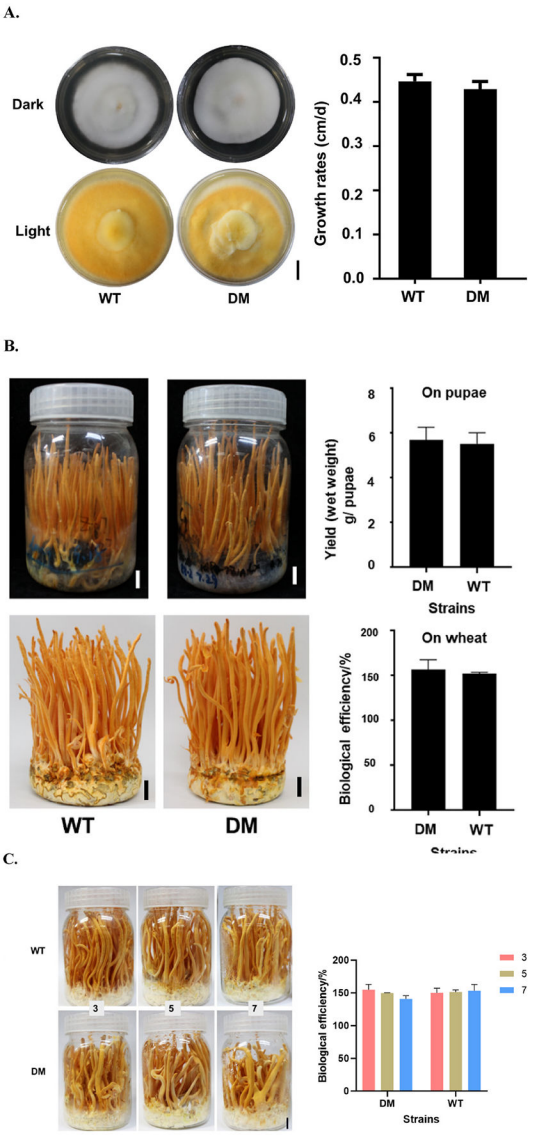

Fig. 5.

Growth and development of *ΔCmustYb-CmustYa* and WT strains (A) Colony morphology and growth rates observed after incubation on PDA medium; Light: exposed to 12 h/12 h white light/dark conditions for 4 d. (B) Fruiting bodies, yield and biological efficiency of *ΔCmustYb-CmustYa* and WT strains cultivated on *A. pernyi* and wheat media. For the cultivation on *A. pernyi*, cuticle-bypassing infection by injection of conidia per pupa was used. (C) The stability of continuous passage of *ΔCmustYb-CmustYa* strain. 3, 5 and 7 represented the passage number after plasmid loss. WT was *C. militaris* strain CGMCC 3.16320; DM was *ΔCmustYb-CmustYa* strain; A, B, C: Bar = 1 cm.

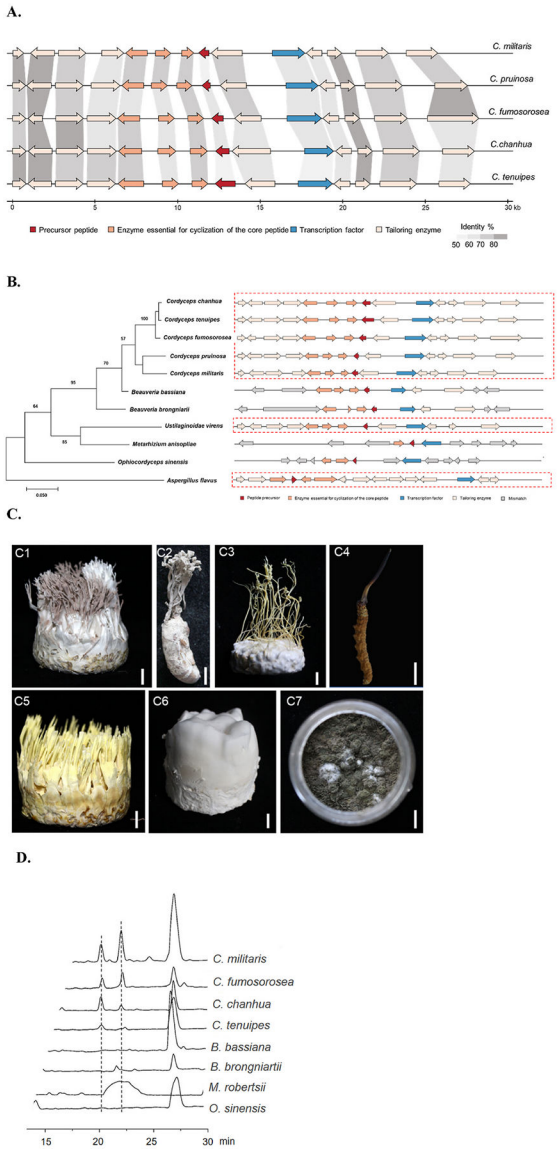

Fig. 6.

Putative ustiloxin BGCs and production of ustiloxin in different *Cordyceps* species (A) Annotations and syntenies of putative ustiloxin BGCs of *C. militaris* (GenBank: GCA_000225605.1), *C. pruinose* (GenBank: GCA_003025255.1), *C. fumosorosea* (GenBank: GCA_001636725.1), *C. chanhau* (GenBank: GCA_002968875.1) and *C. tenuipes* (GenBank: GCA_003025305.1). The genes were represented by horizontal arrows and homologous genes with the same function were color-coded. The sequence identity was shown by boxes with different gray levels. (B) Phylogeny of selected *Cordyceps* sensu lato species and the presence of putative ustiloxin BGCs. Horizontal arrows represent the homologous genes that were color-coded the same as in (A). The phylogeny of selected fungi was inferred with ITS alignments using RAxML under a GTR model. (C) Samples of different *Cordyceps* sensu lato species. C1: *C. fumosorosea*; C2: *C. chanhua*; C3: *C.*

tenuipes; C4: *O. sinensis*; C5: *B. bassiana*; C6: *B. brongniartii*; C7: *M. robertsii*. Bar = 1 cm. (D) HPLC profiles of ustiloxins in different *Cordyceps* species.